Silica Mineralization

DOI: 10.1002/anie.200904494

Synthesis of a DNA–Silica Complex with Rare Two-Dimensional Square *p4mm* Symmetry**

*Chenyu Jin, Lu Han, and Shunai Che**

Studying genetic material to control the two- and three-dimensional packing of biomolecular-scale building blocks into well-defined meso- and macroscopic structures is useful for understanding the mechanisms involved in living organisms, and assists application in biotechnology, nanotechnology, and materials chemistry.[1] Meters of genetic material are naturally packed into compact structures by a variety of methods that are optimized for specific requirements.[2,3] Although many forms of counterion-induced DNA liquid crystals (LCs), such as chiral nematic, uniaxial columnar, and higher-ordered columnar phases,[4–9] as well as supramolecular-directed DNA LCs with lamellar and columnar phases,[10–12] have been studied extensively, the packing behavior of DNA in vivo is not fully understood, and structures mimicking silica mineralization in vitro remain unresolved.

Herein we report the synthesis of a DNA–silica complex (DSC) with a rare two-dimensional (2D) square *p4mm* structure (hereafter denoted *p4mm*), together with a new approach for the structural analysis of DNA liquid-crystal templated mesophases by electron microscopy. By exploiting the cooperative effects of a quaternary ammonium silane, which acts both as a DNA condensing agent through the positively charged quaternary ammonium group and stabilizes silica mineralization by co-condensing with the silica source, *p4mm* and 2D hexagonal *p6mm* DSCs were synthesized at different DNA concentrations, giving rise to a new DNA LC phase diagram. According to the results of simulations based on Kornyshev–Leikin theory[13,14] and previous reports on cation-crystallized DNA,[9,15,16] the small interaxial separation of about 25 Å formed upon quaternary ammonium phosphate electrostatic "zipping" along the DNA–DNA contacts and the silica wall formed between DNA strands in diagonal positions are considered to be optimal for formation of the *p4mm* structure.

In general, DNA is not capable of directing surface deposition of silica to form a DNA–silica complex because silicate is negatively charged in the pH range of 4.3–11.9 needed to maintain the double-helix configuration of DNA.[17] Here we attempted to synthesize a DSC by using the cooperative effects of *N*-trimethoxysilylpropyl-*N*,*N*,*N*-trimethylammonium chloride (TMAPS).[18] The positively charged quaternary ammonium group acts as a condensing agent for DNA, and the silane site is co-condensed with a silica source, for example, tetraethoxysilane (TEOS), for subsequent assembly of the silica framework. The trimethylene groups of TMAPS covalently tether the silicon atoms incorporated into the framework to the cationic ammonium groups regardless of the type of charge on the silicate. We investigated the packing behavior of DNA in DSCs by varying both the DNA concentration and the TMAPS/DNA molar ratio under ambient conditions of neutral pH and room temperature, and we found that varying these parameters allows the DNA interaxial separation to be controlled and consequently promotes formation of various LC phases (vide infra for formation mechanism). Owing to framing of the DNA by a rigid silica wall, formation of DSCs facilitates structural analysis of the DNA LC by electron microscopy, which provides a wealth of information not only from reciprocal space (diffraction) but also in real space (image).

The sonicated DNA ranging in length from 100 to 500 bp used in this study was confirmed by 1% agarose gel electrophoresis (Supporting Information, Figure S1). Homogeneous solutions were formed by addition of TMAPS to aqueous DNA solutions of different concentrations at room temperature. Next, TEOS was added to the mixed solution of DNA and TMAPS. The oil drop of TEOS gradually disappeared, and the solution became cloudy and highly dense. We found that condensation of TMAPS and TEOS is unusually fast at higher DNA concentration, considering the ambient solution conditions of neutral pH and room temperature. After four days, the powder product was recovered by centrifugation and dried at 40 °C under vacuum.

Small-angle X-ray scattering (SAXS) patterns of the DSCs are shown in Figure 1 as a function of increasing DNA concentration. At the highest DNA concentration of 1.0 mg mL^{-1}, two well-resolved

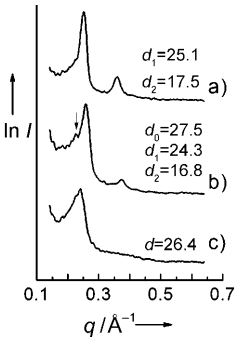

Figure 1. SAXS patterns of DSCs synthesized at DNA concentrations of 1.0 (a), 0.5 (b), and 0.1 (c) mg mL^{-1}, respectively. The molar composition of the reaction mixture was DNA:TMAPS:TEOS:H_2O = *x*:6:15:18333. The samples were synthesized under static conditions at 25 °C for four days.

[*] C. Jin,[+] L. Han,[+] Prof. S. Che
School of Chemistry and Chemical Engineering
State Key Laboratory of Metal Matrix Composites
Shanghai Jiao Tong University
800 Dongchuan Road, Shanghai, 200240 (P. R. China)
Fax: (+86) 215-474-2852
E-mail: chesa@sjtu.edu.cn

[+] These authors equally contributed to this work.

[**] We acknowledge the support of the National Natural Science Foundation of China (Grant No. 20890121 and 20821140537) and the 973 project (2009CB930403) of China.

Supporting information for this article is available on the WWW under http://dx.doi.org/10.1002/anie.200904494.

peaks appeared in the range of $q = 0.2$–0.4 Å^{-1} with a d-spacing ratio of $q_0/q_1 = \sqrt{2}$, which is rare in previously reported DNA liquid-crystalline phases. From this ratio, a 2D square lattice can be assumed, and the two peaks can be indexed to 10 and 11 reflections with a unit-cell parameter of $a = 25$ Å. There are three possible plane groups of a 2D square lattice: *p*4, *p*4*mm*, and *p*4*gm*. However, the SAXS data are insufficient to solve the structure. The correct plane group can be determined by HRTEM analysis (vide infra). At the lowest DNA concentration of 0.1 mg mL^{-1}, the sample had only one broad peak with a d spacing of 26 Å. The sample synthesized at the intermediate DNA concentration of 0.5 mg mL^{-1} displayed three peaks: the q_0 peak is in a position similar to that of the sample synthesized at 0.1 mg mL^{-1}, and q_1 and q_2 coincide with the two peaks observed in the sample synthesized at 1.0 mg mL^{-1}, that is, this sample could be a mixture of two phases.

Scanning electron microscopy (SEM; Figure 2a$_1$, see also Supporting Information, Figure S2a for a low-magnification image) revealed that the DSC synthesized at high DNA concentration was composed of platelets uniform in size with an average diameter of about 800 nm and a uniform thickness of about 100 nm. The platelet thickness is equal to the average length of DNA used here. Figures 2a$_2$ and 2a$_3$ show typical HRTEM images and corresponding Fourier diffractograms (FDs) taken from the top and side of the platelet, which reveal a 2D structure. The highest order of rotation is fourfold, and the axes of reflection are inclined to each other by 45°, indicative of *p*4*mm* symmetry. Thus, the two peaks of the SAXS pattern can be concluded to be 10 and 11 reflections based on the *p*4*mm* plane group. The unit-cell parameter calculated from the TEM image is $a = 23$ Å, smaller than that obtained from the SAXS results, which may be due to an error in the TEM observations. The crystal was found to contain local fluctuations and defects, which may be introduced by edge or screw dislocations due to the nonuniform distribution of lengths of the DNA molecules (Supporting Information, Figure S3). More particle images are shown in Figure S4 of the Supporting Information. An electrostatic-potential map (Figure 2a$_4$) of the structure was constructed by taking the inverse Fourier summation of the crystal structure factors[19] (Supporting Information, Table S1). It shows that an extremely thin silica wall (or almost no wall) was formed between the two nearest DNA strands.

The DSC synthesized at low DNA concentration was composed of uniform platelets of about 500 nm in diameter and 50–100 nm in thickness (Figure 2b$_1$, see also Supporting Information, Figure S2b for a low-magnification image), which is equal to the DNA length, similar to the platelets with *p*4*mm* symmetry. The HRTEM images and corresponding FDs (Figures 2b$_2$ and 2b$_3$) of this sample show *p*6*mm* symmetry with a unit-cell parameter of $a = 29$ Å. A thick silica wall was formed, as seen in the electrostatic-potential map (Figure 2b$_4$). The crystal structure factors are listed in Table S2 of the Supporting Information.

In the samples synthesized at intermediate DNA concentrations, particles with both *p*6*mm* and *p*4*mm* structures were found (Supporting Information, Figure S5). The interaxial separations of *p*4*mm* and *p*6*mm* in the same sample are about 23 Å and about 28 Å, respectively, similar to those of the two pure samples. The interaxial separations of the *p*4*mm* structures observed in the mixed samples are in the range of

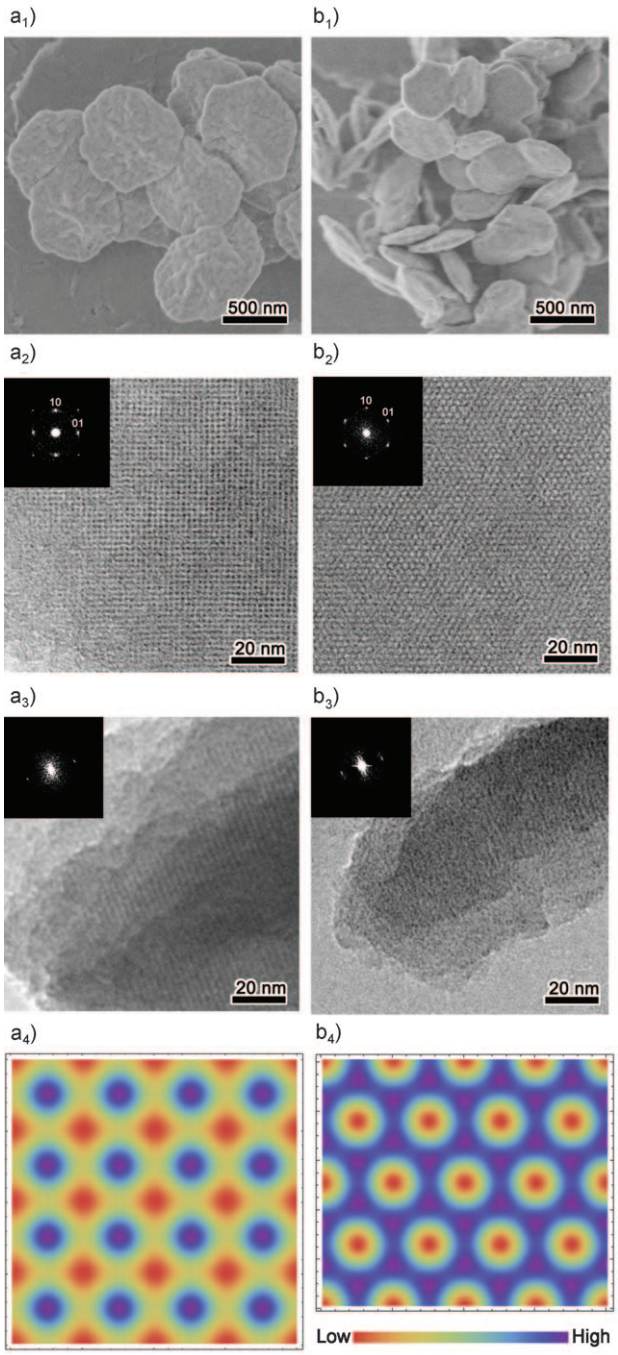

Figure 2. Morphologies and structures of DSCs with *p*4*mm* (a) and *p*6*mm* symmetry (b) corresponding to Figure 1a and c, respectively. a$_1$ and b$_1$) SEM images showing the microscopic features of these samples. The samples were observed without any metal coating. a$_{2,3}$ and b$_{2,3}$) TEM images taken from the top and side of the platelet and the corresponding Fourier diffractograms, showing the ordered 2D structure. a$_4$ and b$_4$) Electrostatic-potential maps, clearly showing that the interaxial separation in the *p*4*mm* structure is much smaller than that in the *p*6*mm* structure.

23–25 Å, smaller than those of the *p6mm* structures, which were in the range of 28–31 Å.

The phase diagram of the DSC (Figure 3a) shows three types of structure: 1) DNA and DNA superstructures forming transcribed mesoporous fibers (Supporting Information, Figure S6) and 2) *p4mm* and 3) *p6mm* structures. These structures were synthesized at lower TMAPS/DNA molar ratios and at higher (1.0 mg mL^{-1}) and lower DNA concentrations (0.1 mg mL^{-1}), respectively. Intermediate DNA concentrations (0.2 and 0.5 mg mL^{-1}) resulted in mixed phases with both *p4mm* and *p6mm* structures. This result indicates that small amounts of countercations were insufficient to condense the DNA into packed structures. Both higher DNA concentrations and higher TMAPS concentrations were favorable for formation of *p4mm* structures. Disordered structures were synthesized at TMAPS/DNA molar ratios larger than 100, and an irregular monolith-like morphology was formed at DNA concentration higher than 1.0 mg mL^{-1}. The phase diagrams are dependent on the H_2O/TEOS and TEOS/TMAPS molar ratios, temperature, and synthesis time. The DSC can be synthesized over a wide temperature range of 5–50 °C. Smaller DNA molecules (< 50 bp) led to the formation of spherical particles (Supporting Information, Figure S7). A combination of DNA longer than 500 bp and TMAPS resulted in the formation of diverse porous silica fibers of DNA[20] and irregular silica–DNA aggregates (Supporting Information, Figure S8). The interaxial separations *R* obtained from the SAXS patterns decreased with increasing DNA concentration and showed a slight increase with increasing TMAPS/DNA molar ratio (Figure 3b). It is noteworthy that the *R* value of the *p4mm* (24–26 Å) structure is significantly smaller than that of the *p6mm* structure (29–31 Å), that is, the structural transition depends on the interaxial separation of the DNA molecules.

DNA molecules with a large interaxial separation can be modeled as uniformly charged cylinders.[21] However, the net charge distribution on the molecules is not homogeneous, and this dramatically changes the interaction potential at intermediate distances.[22] The phase behavior of columnar DNA packing depends on both the interaxial distance and on special requirements for the azimuthal orientation.[14] In the interacting DNA–DNA system, 2D hexagonal, 3D hexagonal, and orthorhombic DNA LC phases with different interaxial separations of 29.0–31.5, 23.7–29.0, and 18.1–23.1 Å, respectively, were induced by various counterions.[9] However, in both liquid-crystal and DNA-packing systems, it is very rare to encounter square columnar symmetry,[23] since long-range orientational order is always formed by maximizing the interaction energy and minimizing the excluded volume.[24] It has been reported that DNA square packing symmetries with large interaxial distances (32–39 Å) can be directed by supramolecular templating.[12] Here it was speculated that the *p4mm* structure with a small interaxial separation induced by a small counterion depends on a specific azimuthal orientation for close DNA–DNA interaction, which was conjectured on the basis of similar azimuthal ordering.[14]

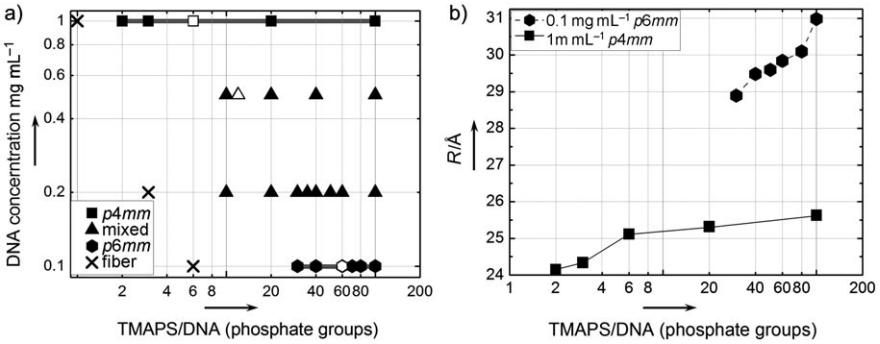

Figure 3. Phase behavior and structural factors. a) Phase diagram established by SAXS patterns and HRTEM analyses of 27 samples synthesized with varying DNA concentrations and TMAPS/DNA molar ratios. Each synthesis gel mixture had an H_2O/TEOS molar ratio of 1222:1. Empty symbols correspond to the samples shown in Figure 1. b) Interaxial separation *R* versus TMAPS/DNA molar ratio with constant DNA concentration for the samples indicated by gray lines in (a). Interaxial separations of the mixed-phase samples were not calculated, because not every SAXS pattern produced clear peaks indexed to two phases.

We propose that when TMAPS is added to the DNA solution, a helical arrangement of the cationic quaternary ammonium groups could form in the minor and major grooves of the DNA through hydrophobic interactions between the silane and grooves (Figure 4a and b), similar to the interaction between DNA and most cations.[25,26] During the synthetic reaction, the alkoxy silane sites of TMAPS will be hydrolyzed by small amounts of water in the grooves, gradually moved to the DNA surface, and then co-condensed with TEOS to form the silica framework (Figure 4c). A small DNA–DNA interaxial separation would be obtained at higher concentrations by the formation of an electrostatic "zipper" (II–III) with interactions between the negatively charged strands and positively charged grooves of opposing molecules.[13–16] An ideal zipper requires the mutual azimuthal orientation to be 72–108°. This angle can be obtained in geometrical calculations based on the B-DNA structure when the two strands are separated by an azimuthal angle of about 144° (Supporting Information, Figure S9). As shown in Figure 4d, a square lattice with any mutual orientation angle can be reasonably conjectured on the basis of the lattice sums, as long as the diagonal distance is optimized to a mutual azimuthal orientation angle of 0° (I–III).

For the square DSC with an interaxial separation of 24–26 Å, it can be determined that the interaxial separation between DNA strands in diagonal positions is 34–37 Å. The mutual orientation of the angles in the diagonal position would be negated by the larger distance[21] and by formation of the silica wall, which prevents their interaction and leads to formation of the *p4mm* structure. On the other hand, the small interaxial separation would facilitate silicate condensation, and this is why fast condensation was observed at higher

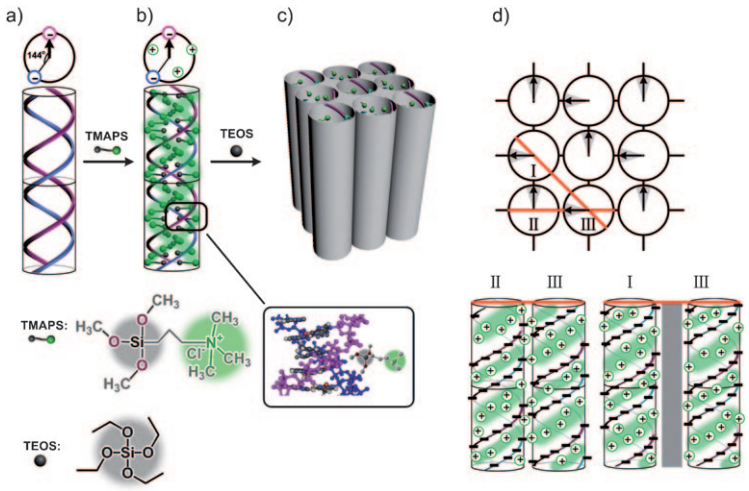

Figure 4. Schematic illustration of the mechanism of formation of a DSC with 2D square structure. a) B-DNA structure. A plane perpendicular to the parallel axes of the DNA molecule; DNA strands are depicted as circles. The azimuthal width of the minor groove is 144° (0.8 π). b) Interaction between DNA and TMAPS. The hydrophobic alkoxy silane group of TMAPS binds preferentially to both the hydrophobic minor and major grooves of DNA, and its cationic quaternary ammonium groups emerge on the surface to form distinct cationic helical strands in both the minor and major grooves as continuous line charges, in a manner similar to the phosphate backbone. c) A square lattice in which a silica wall is framed by four other DNA columns. d) The gray areas (72–108°) indicate the possible azimuthal orientations of DNA molecules required by an ideal zipper. As an example, 90° is illustrated, indicated by the black arrows. I–II: The surface charge pattern of two model DNA molecules. The negatively charged strands come close to the positively charged grooves of the opposing molecule to form an electrostatic zipper. III–I: Interaction between two DNA strands in diagonal positions with an azimuthal orientation angle of 0°. (The DNA ball-and-stick model was generated from the coordinates of MMDB ID: 74408[27]).

DNA concentration. The large distance at lower DNA concentrations and formation of silica surrounding their surface would make the DNA column a uniform cylinder, as well as resulting in hexagonal close packing (Supporting Information, Figure S10).

As far as we know, this is the first example of DNA liquid-crystal silica mineralization and the first synthesis of a DNA 2D square packing with unusually small interaxial separation. The specific effects of cation distribution, silica polymerization, DNA interaxial separation, and DNA-helix orientation have given rise to a new DNA liquid-crystal phase system. This result, together with structural analysis by electron microscopy, opens new horizons for the study of the physical theory of DNA assembly, biological macromolecular interactions, and assembly of functional metamaterials.

Experimental Section

DNA assays: The DNA used in this work was DNA sodium salt from herring testes (Sigma), formally listed as Type XIV. The DNA was dissolved in deionized water by stirring at room temperature (ca. 298 K) for 3–4 h, with a final concentration of 1.0 mg g^{-1} H_2O. The solution was then treated with an ultrasonic cell crusher at 400 W for 2.5 h. Agarose gel electrophoresis was performed with 1 % agarose at 130 V.

Preparation of DSCs: DSCs were synthesized from sonicated DNA ranging from 100 to 500 bp in length, TMAPS, and TEOS at neutral pH and room temperature. In a typical synthesis, TMAPS (87.9 mg, 50 % in methanol) was added to the DNA solution (1 mg mL^{-1}, 10 mL) with stirring at room temperature. TEOS (90.6 mg) was added to the mixed solution with vigorous stirring at room temperature, and the mixture was allowed to react at room temperature under static conditions for 4 d. The powder products were recovered by centrifugal separation and dried at 40 °C under vacuum.

Characterization: SAXS patterns were recorded on a Nanostar U small-angle X-ray scattering system (Bruker, Germany) with $Cu_{K\alpha}$ radiation (40 mV, 35 mA). The microscopic features of all samples were observed by SEM (JEOL JSM-7401F). To observe the true external surface, the samples were studied without any metal coating. An accelerating voltage of 1 kV (resolution: ca. 1.4 nm) was chosen for all mesoporous silica samples. HRTEM was performed with a JEOL JEM-2100 microscope operating at 200 kV ($C_s = 1.0$ mm, point resolution 2.3 Å). Images were recorded with a KeenView CCD camera (resolution 1376 × 1032 pixels, pixel size 6.45 × 6.45 μm) at 50 000–120 000 times magnification under low-dose conditions.

Received: August 12, 2009
Published online: November 7, 2009

Keywords: DNA structures · liquid crystals · mineralization · phase diagrams · silica

[1] H. Cölfen, S. Mann, *Angew. Chem.* **2003**, *115*, 2452–2468; *Angew. Chem. Int. Ed.* **2003**, *42*, 2350–2365.
[2] V. A. Bloomfield, *Curr. Opin. Struct. Biol.* **1996**, *6*, 334–341.
[3] F. Livolant, A. Leforestier, *Prog. Polym. Sci.* **1996**, *21*, 1115–1164.
[4] T. E. Strzelecka, M. W. Davidson, R. L. Rill, *Nature* **1988**, *331*, 457, 457–460.
[5] F. Livolant, A. M. Levelut, J. Doucet, J. P. Benoit, *Nature* **1989**, *339*, 724–726.
[6] M. Nakata, G. Zanchetta, B. D. Chapman, C. D. Jones, J. O. Cross, R. Pindak, T. Bellini, N. A. Clark, *Science* **2007**, *318*, 1276–1279.
[7] J. Pelta, Jr., D. Durand, J. Doucet, F. Livolant, *Biophys. J.* **1996**, *71*, 48–63.
[8] N. Sundaresan, C. H. Suresh, T. Thomas, T. J. Thomas, C. K. S. Pillai, *Biomacromolecules* **2008**, *9*, 1860–1869.
[9] D. Durand, J. Doucet, F. Livolant, *J. Phys. II Fr.* **1992**, *2*, 1769–1783.
[10] S. Chesnoy, L. Huang, *Annu. Rev. Biophys. Biomol. Struct.* **2000**, *29*, 27–47.
[11] I. Koltover, T. Salditt, J. O. Radler, C. R. Safinya, *Science* **1998**, *281*, 78–81.
[12] H. M. Evans, A. Ahmad, K. Ewert, T. Pfohl, A. Martin-Herranz, R. F. Bruinsma, C. R. Safinya, *Phys. Rev. Lett.* **2003**, *91*, 075501.
[13] A. A. Kornyshev, S. Leikin, *Phys. Rev. Lett.* **1999**, *82*, 4138–4141.
[14] H. M. Harreis, C. N. Likos, H. Lowen, *Biophys. J.* **2003**, *84*, 3607–3623.
[15] A. A. Kornyshev, D. J. Lee, S. Leikin, A. Wynveen, S. B. Zimmerman, *Phys. Rev. Lett.* **2005**, *95*, 148102.
[16] H. Millonig, J. Pous, C. Gouyette, J. A. Subirana, J. L. Campos, *J. Inorg. Biochem.* **2009**, *103*, 876–880.

[17] M. Numata, K. Sugiyasu, T. Hasegawa, S. Shinkai, *Angew. Chem.* **2004**, *116*, 3341 – 3345; *Angew. Chem. Int. Ed.* **2004**, *43*, 3279 – 3283.
[18] S. Che, A. E. Garcia-Bennett, T. Yokoi, K. Sakamoto, H. Kunieda, O. Terasaki, T. Tatsumi, *Nat. Mater.* **2003**, *2*, 801 – 805.
[19] Y. Sakamoto, M. Kaneda, O. Terasaki, D. Y. Zhao, J. M. Kim, G. Stucky, H. J. Shin, R. Ryoo, *Nature* **2000**, *408*, 449 – 453.
[20] C. Jin, H. Qiu, L. Han, M. Shu, S. Che, *Chem. Commun.* **2009**, 3407 – 3409.
[21] G. S. Manning, *Q. Rev. Biophys.* **1978**, *11*, 179 – 246.
[22] A. A. Kornyshev, S. Leikin, *J. Chem. Phys.* **1997**, *107*, 3656 – 3674.
[23] B. Chen, X. Zeng, U. Baumeister, G. Ungar, C. Tschierske, *Science* **2005**, *307*, 96 – 99.
[24] R. Hołyst, P. Oswald, *Macromol. Theory Simul.* **2001**, *10*, 1 – 16.
[25] N. V. Hud, M. Polak, *Curr. Opin. Struct. Biol.* **2001**, *11*, 293 – 301.
[26] B. C. Feuerstein, L. D. Williams, H. S. Basu, L. J. Marton, *J. Cell. Biochem.* **1991**, *46*, 37 – 47.
[27] S. Arai, T. Chatake, T. Ohhara, K. Kurihara, I. Tanaka, N. Suzuki, Z. Fujimoto, H. Mizuno, N. Niimura, *Nucleic Acids Res.* **2005**, *33*, 3017 – 3024.

